

On the Equivalence Point for Ammonium (De)protonation during Its Transport through the AmtB Channel

David L. Bostick and Charles L. Brooks III

Department of Molecular Biology and Center for Theoretical Biological Physics, The Scripps Research Institute, La Jolla, California 92037

ABSTRACT Structural characterization of the bacterial channel, AmtB, provides a glimpse of how members of its family might control the protonated state of permeant ammonium to allow for its selective passage across the membrane. In a recent study, we employed a combination of simulation techniques that suggested ammonium is deprotonated and reprotonated near dehydrative phenylalanine landmarks (F107 and F31, respectively) during its passage from the periplasm to the cytoplasm. At these landmarks, ammonium is forced to maintain a critical number (~ 3) of hydrogen bonds, suggesting that the channel controls ammonium (de)protonation by controlling its coordination/hydration. In the work presented here, a free energy-based analysis of ammonium hydration in dilute aqueous solution indicates, explicitly, that at biological pH, the transition from ammonium (NH_4^+) to ammonia (NH_3) occurs when these species are constrained to donate three hydrogen bonds or less. This result demonstrates the viability of the proposal that AmtB indirectly controls ammonium (de)protonation by directly controlling its hydration.

Received for publication 18 March 2007 and in final form 6 April 2007.

Address reprint requests and inquiries to Charles Brooks, E-mail: brooks@scripps.edu.

AmtB exists in the membrane as a homotrimer. Each monomer of this protein forms a channel that passively transports ammonium (NH_4^+) in the form of its “gas” ammonia (NH_3) intermediate across the membranes of bacteria; for conciseness we will henceforth refer to both NH_4^+ and NH_3 species, together, as Am. Structural models of AmtB resulting from x-ray diffraction (1,2) have provided initial configurations for a plethora of computational (3–10,13) studies aimed at understanding this channel’s mechanistic aspects and implications for homologous human counterparts.

The center of an AmtB monomer forms a narrow hydrophobic pore (lumen) connecting cytoplasmic and periplasmic vestibules, both accessible to aqueous solution. Diffraction studies revealed an NH_4^+ binding site in the cytoplasmic vestibule (site Am1 (1,2)) where the cation donates hydrogen bonds to the backbone carbonyl group of A162, the side-chain hydroxyl oxygen of S219, and ~ 2 –3 water molecules (3,5,7). Aromatic groups (F107 and F215) form a floor for site Am1, capping the hydrophobic lumen to help prevent entrance of water from the periplasm (see Fig. 1). These aromatic groups rotate at low free energy cost to allow translocation of Am (3,5,7) under the influence of an electrochemical gradient.

In the presence of AmSO_4 , the x-ray structure (1) displayed three luminal binding sites (Am2, Am3, and Am4—see Fig. 1 A), where Am interacts closely with His residues (H168 and H318). Calculations of the apparent pK_a of luminal Am (3,10) indicate that these sites may only be occupied by neutral NH_3 . As such, it would appear that the disallowance of permanently charged species in the lumen is the most Am-selective feature of AmtB. An aromatic group (F31) just below site Am4 helps to prevent hydration of the lumen, and provides a low free energy barrier for NH_3 passage to the cytoplasmic vestibule (Fig. 1, A and B). Just below the lumen, a fifth site (Am5) was revealed by a

molecular dynamics (MD) study (3). At this site, calculations of the apparent pK_a (3) suggest Am must exist in its protonated form, where it donates hydrogen bonds to a carboxyl oxygen of D313, the hydroxyl oxygen of S263, and surrounding water (Fig. 1, A and B).

Combining knowledge of experimental and computational results (1–3,10), it appears that AmtB deprotonates NH_4^+ between sites Am1–2, and reprotonates NH_3 between sites Am4–5 to allow Am flux toward the cytoplasm. However, it is difficult to determine, experimentally, how the channel controls these (de)protonation events. Computational studies, though they should help clarify the (de)protonation mechanism, have proposed disparate explanations (3–5,7). Lin et al. (5) and Nygaard et al. (7) both proposed that a highly conserved Asp residue (D160), whose mutation is known to destroy AmtB’s transport capability (11), plays a key role in NH_4^+ deprotonation. Lin et al. (5) observed that water forms a hydrogen bonded network between NH_4^+ at Am1 and the carboxylate of D160. This led them to suggest that the charged carboxylate drives deprotonation at site Am1, and accepts a proton donated by NH_4^+ using hydronium as an intermediate. On the other hand, Nygaard et al. (7) proposed that deprotonation occurs near site Am2, after NH_4^+ moves from Am1 across the stacked (F107/F215) aromatic moieties. In this configuration, it was suggested that NH_4^+ donates a proton to D160 via the backbone carbonyl group of A162 and the amide N–H of G163 using an imidic acid mechanism.

Luzhkov et al. (10) presented results that would suggest that D160 does not function as a proton acceptor. Rather, their calculations showed that the apparent pK_a of D160’s carboxylate is downshifted (from its standard value of ~ 3.9) by

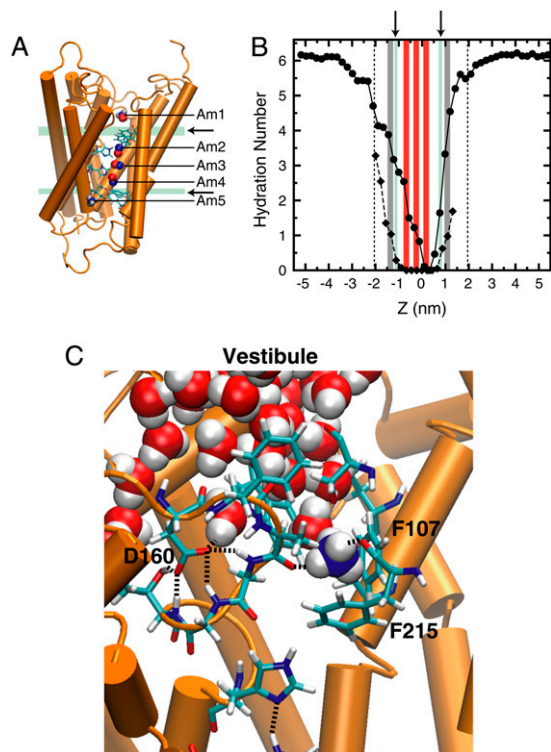


FIGURE 1 (A) Synopsis of binding sites and deprotonation regions. Some helices have been removed from the protein (orange) to allow visibility of the binding sites. The positions of the x-ray sites are shown as red spheres, and Am binding sites derived from simulation (3) are shown as either blue spheres (for NH_3) or blue spheres with white hydrogen atoms (for NH_4^+). (De)protonation regions are marked in green (see arrows). The periplasmic and cytoplasmic (de)protonation regions coincide with the phenyl groups of F107 and F31, respectively. (B) Hydration of NH_3 (diamonds with dashed line) and NH_4^+ (circles with solid line) as a function of the transport axis (Z). The origin coincides with the center of mass of the AmtB trimer ($Z > 0$ is the periplasmic membrane leaflet, and $Z < 0$ is the cytoplasmic). Dotted lines denote lipid phosphate positions, gray bars mark sites Am1 and Am5, red bars mark sites Am2-4, and green bars (see arrows) mark (de)protonation regions (Am equivalence points). (C) Proposed equivalence point for NH_4^+ deprotonation near the periplasmic end of the lumen. Here, NH_4^+ is stripped to three hydrogen bonds (donated to carbonyl groups of A162 and F215 and one water), and has full access to vestibular water, continuously connected to bulk solution, to allow the escape of a proton to the bulk in the form of hydronium ion.

0.3–5.1 units when site Am1 is unoccupied. When NH_4^+ occupies Am1, the apparent pK_a of D160 shifts even further downward by 9.2 units, making its protonation effectively impossible. Our own results (3), as well as those of Luzhkov et al., showed that D160 is engaged in persistent hydrogen bonds with the protein, and that the negative charge of D160 stabilizes Am in its protonated form, shifting its apparent pK_a upward by ~ 4 units. Taken together, these results indicate that the importance of D160, as evidenced by mutational studies (11), is more likely due to recruitment of NH_4^+ from the periplasm and stabilizing its binding at site Am1 rather

than accepting a proton as suggested by Lin et al. and Nygaard et al.

Recently we utilized a combination of MD simulation techniques (3), showing that the equivalence points for Am (de)protonation coincide with the periplasmic and cytoplasmic phenyl groups of F107 and F31, respectively (Fig. 1 A). Near these specific regions, Am was seen to be stripped to ~ 3 or fewer hydrogen bonds (Fig. 1 B). At the periplasmic (de)protonation site (Fig. 1, B and C), near F107, NH_4^+ may donate two hydrogen bonds to protein and ~ 1 to water. At the cytoplasmic (de)protonation site, it appears that water provides all ~ 3 hydrogen bonds (Fig. 1 B). Given that, a), water ionizes more easily than a carbonyl group, b), the carboxylate of D160 is persistently engaged in hydrogen bonds with the protein that shift its apparent pK_a downward (10), and c), at both equivalence points, Am has full access to vestibular water, we proposed that water is the only plausible proton acceptor for NH_4^+ . After accepting this proton, it is most likely that the proton escapes to the periplasm in the form of hydronium.

Our previous study showed a clear correlation between the protonated form of Am and the number of available hydrogen bonds. However, we did not directly demonstrate that the channel need only constrain Am to ~ 3 or fewer hydrogen bonds to deprotonate NH_4^+ . Such a demonstration would require a computational experiment that rules out other effects, such as the local electric field imposed by the channel at the (de)protonation regions. To address this issue in a most general way, we performed simulations of both NH_4^+ and NH_3 in dilute aqueous solution (see Supplementary Material). These simple simulations allowed us to isolate and directly probe the dependence of Am's apparent pK_a on coordination (hydrogen-bond) number.

In the spirit of previous work (12), we performed a free energy characterization of solute (NH_4^+ and NH_3) hydration preferences based upon population analysis from MD trajectories. From this analysis, we derived the apparent pK_a of Am as a function of its coordination number as follows (see Supplementary Material):

$$\text{pK}_a(N_p, N_{dp}) = \text{pK}_a^{\text{bulk}} - \frac{1}{2.303} \ln \left(\frac{P_{dp}(N_{dp})}{P_p(N_p)} \right),$$

where, $P_x(N_x)$ is the probability that the coordination (hydrogen bond) number around Am in the state x is N_x ($x = dp$ for “deprotonated” Am, or NH_3 , and $x = p$ for “protonated” Am, or NH_4^+), and $\text{pK}_a^{\text{bulk}}$ is the pK_a of NH_4^+ in bulk aqueous solution.

The resulting apparent pK_a profile is shown in Fig. 2. This analysis indicates that if a local environment provides only ~ 3 or fewer hydrogen bonds, Am will be favored in its deprotonated form, NH_3 . The equivalence point between NH_4^+ and NH_3 , itself, appears to occur near the midpoint between three and four available acceptors. In tandem with previous results (3,10), this indicates that the functional role of D160 is to allow for AmtB's structural and electrostatic ability to recruit NH_4^+ from the periplasm, and not to drive the

deprotonation of NH_4^+ . Since Fig. 2 describes the local pK_a of Am in an isotropic medium—that of pure water—the analysis shows that loss of a proton from NH_4^+ occurs with ~ 3 hydrogen bonds regardless of any external field provided by AmtB at the calculated equivalence points shown in Fig. 1. The result we show here appears to be independent of the force field chosen to describe Am or water (Supplementary Material, Fig. S1), and suggests that AmtB's control over Am hydration, or equivalently, the number of hydrogen bonds, is the sole control over (de)protonation provided by the protein, as we have suggested (3).

It is also interesting to consider this result in light of a recent study suggesting a stable water chain can enter the lumen (13) from the cytoplasm. If, indeed, this occurs, NH_4^+ might occupy the lumen more favorably than previously thought. Our previous work (3) suggested that if NH_4^+ enters the lumen, it may be hydrated by as many as 2–3 water molecules (Fig. 1 B). However, the data presented here (Fig. 2) indicate Am will exist as NH_3 if only three hydrogen bond

partners are provided. Thus, the (de)protonation sites we suggest (Fig. 1 and Bostick and Brooks (3)) can still hold true despite a hydrated pore. Also, the preference of NH_3 for three-fold (or less) coordination forces us to consider the possibility that NH_3 and H_2O might coexist in a confined luminal environment. We suggest that future computational study aimed at determining Am's protonation state in a hydrated lumen may shed light on this issue.

SUPPLEMENTARY MATERIAL

An online supplement to this article can be found by visiting BJ Online at <http://www.biophysj.org>

ACKNOWLEDGMENTS

This material is based upon work supported by the National Science Foundation (NSF) under grant No. 0434578. Additional NSF support (PHYS0216576 and MCB-0413858) and support from the National Institutes of Health (RR06009) are also acknowledged.

REFERENCES and FOOTNOTES

1. Khademi, S., J. O'Connell III, J. Remis, Y. Robles-Colmenares, L. J. W. Miercke, and R. M. Stroud. 2004. Mechanism of ammonia transport by Amt/Mep/Rh structure of AmtB at 1.35 Å. *Science*. 305:1587–1594.
2. Zheng, L., D. Kostrewa, Bernèche, F. K. Winkler, and X.-D. Li. 2004. The mechanism of ammonia transport based on the crystal structure of AmtB of *Escherichia coli*. *Proc. Natl. Acad. Sci. USA*. 101:17090–17095.
3. Bostick, D. L. and C. L. Brooks III. 2007. Deprotonation by dehydration: the origin of ammonium sensing in the AmtB channel. *PLoS Comput. Biol.* 3:e22/0001–0015.
4. Ishikita, H., and E.-W. Knapp. 2007. Protonation states of ammonia/ammonium in the hydrophobic pore of ammonia transporter protein AmtB. *J. Am. Chem. Soc.* 129:1210–1215.
5. Lin, Y., Z. Cao, and Y. Mo. 2006. Molecular dynamics simulations on the *Escherichia coli* ammonia channel protein AmtB: mechanism of ammonia/ammonium transport. *J. Am. Chem. Soc.* 128:10876–10884.
6. Liu, Y., and X. Hu. 2006. Molecular determinants for binding of ammonium ion in the ammonia transporter AmtB—a quantum chemical analysis. *J. Phys. Chem. A*. 110:1375–1381.
7. Nygaard, T. P., C. Rovira, G. H. Peters, and M. Ø. Jensen. 2006. Ammonium recruitment and ammonia transport by *E. coli* ammonia channel AmtB. *Biophys. J.* 91:4401–4412.
8. Yang, H., Y. Xu, W. Zhu, K. Chen, and H. Jiang. 2007. Detailed mechanism for AmtB conducting $\text{NH}_4^+/\text{NH}_3$: molecular dynamics simulations. *Biophys. J.* 92:877–885.
9. Callebaut, I., F. Dulin, O. Bertrand, P. Ripoche, I. Mouro, Y. Colin, J.-P. Mornon, and J.-P. Cartron. 2006. Hydrophobic cluster analysis and modeling of the human Rh protein three-dimensional structures. *Transfus. Clin. Biol.* 13:70–84.
10. Luzhkov, V. B., M. Almlöf, M. Nervall, and J. Åqvist. 2006. Computational study of the binding affinity and selectivity of the bacterial ammonium transporter AmtB. *Biochemistry*. 45:10807–10814.
11. Javelle, A., E. Severi, J. Thornton, and M. Merrick. 2004. Ammonium sensing in *Escherichia coli*. *J. Biol. Chem.* 279:8530–8538.
12. Bostick, D., and C. L. Brooks III. 2007. Selectivity in K^+ channels is due to topological control of the permeant ion's coordinated state. *Proc. Natl. Acad. Sci. USA*. In press.
13. Lamoureux, G., M. L. Klein, and S. Bernèche. 2007. A stable water chain in the hydrophobic pore of the AmtB ammonium transporter. *Biophys. J.* 92:L82–L84.

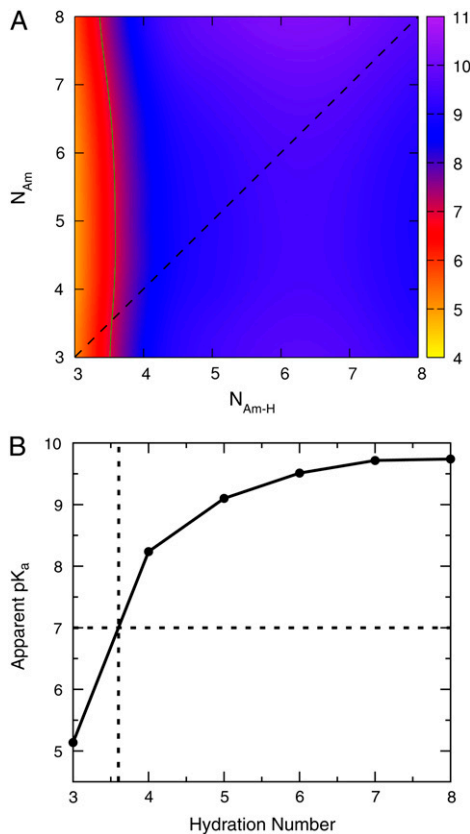


FIGURE 2 (A) Apparent pK_a of Am in a local environment that provides $N_{\text{Am-H}}$ hydrogen bonds for NH_4^+ and N_{Am} hydrogen bonds for NH_3 derived from population analysis of MD trajectories for Am in dilute aqueous solution. The green contour line indicates the equivalence point ($\text{pK}_a = 7$). The diagonal dashed line indicates where $N_{\text{Am-H}} = N_{\text{Am}}$. **(B)** Apparent pK_a of Am for a local hydration environment where $N_{\text{Am-H}} = N_{\text{Am}}$. Note that the equivalence point occurs in an environment providing 3.6 hydrogen bonds or less (see the dotted lines).